Industrial Engineering Journal
ISSN: 0970-2555
Volume : 53, Issue 4, No. 4, April : 2024

WINDS AS WELL AS PHOTOVOLTAIC-BASED HYBRID STAND-ALONE POWER PRODUCTION SYSTEMS

Divyam Saxena M. Tech. Scholar of Electrical Engineering department of FET, Rama University Uttar Pradesh Kanpur 209217
Raghvendra Singh Assistant Professor of Electronic & communication engineering department of FET, Rama University Uttar Pradesh Kanpur 209217 Email id: dsaxena7798@gmail.com

Abstract:
In the present day, electric performs a crucial role in facilitating daily tasks. However, it is sad that many locations lack access to energy due to challenges faced by power grid networks. For the countryside, the optimal solution is to install a local independent power system to supply the necessary electricity for improved quality of life. Diesel generators are predominantly utilized for power generating, however, they are not cost-effective or environmentally friendly due to the escalating price of diesel and the emission of carbon compounds and noise during power generation. An alternate option is to install a stand-alone power system that relies on renewable energy sources. Wind power generation is the most widely used kind of renewable energy, although the use of Photovoltaic power systems is also steadily increasing in society. Integrating two or more renewable systems enhances the reliability of stand-alone power sources. This study presents a proposed hybrid power generation system that combines wind and solar energy sources. The system is designed for standalone use in rural areas. MPPT converters are also incorporated to optimize the utilization of renewable energy sources by achieving the greatest power output. To enhance reliability, the system is equipped with a battery that includes a voltage-based controller. Furthermore, the majority of the distribution loads in a three-phase power system were unbalanced. Therefore, it is essential that there are balancing voltage at the load bus in order to provide high power quality. To provide optimal power quality, a controller is specifically created for the inverter to regulate the single phase voltages and maintain them at their designated value of reference. Comprehensive controllers are created and evaluated in MATLAB Simulink for both balancing and unbalanced loads scenarios. The controllers operate adequately under a range of potential situations.
Keywords: This stand-alone systems includes a PMDC generator, a photovoltaic (PV) an inverter, and uses energy from renewable sources.

1.0 Introduction

In numerous countries worldwide, there are places distant regions where establishing a power grid link is both costly and unfeasible [1-4]. In distant areas where there is no access to electricity, the only available source is a diesel generator. However, this option is not environmentally friendly. To address this issue, we can provide electricity for homes in these areas by implementing a power production system that relies on renewable energy sources [4-5]. The system is referred to as a stand-alone electrical power technology. Wind turbine-based energy production technologies are widely preferred in stand-alone systems. Nevertheless, the windmill electricity production system alone is unable to provide the necessary power to the load. Therefore, we have incorporated the Photovoltaic (PV) system into the wind-based energy generation technology. Furthermore, both sources are reliant on weather conditions and subject to fast fluctuations in their characteristics. Likewise, the load is likewise undergoing quick and frequent changes. In order to store energy during light load conditions, a storage device is necessary. Additionally, an alternative power source is needed to provide the required power during heavy load conditions. These gadgets, namely batteries, are being incorporated into the system to enhance its reliability. These systems are sometimes referred to as stand-alone systems. They consist of a mix of two or more renewable energy sources along with storage devices to enhance reliability. They are extensively utilized for power applications in remote places worldwide. The primary obstacle with this particular stand-alone hybrid energy system is to achieve dependable and consistently high

power quality while also being affordable.

Variable speed wind turbines are highly efficient and capable of capturing additional power from the wind by utilizing MPPT converters. This makes them a popular choice for wind energy applications [4-6]. Similarly, in order to optimize the performance of a photovoltaic (PV) system, it is necessary to employ a Maximum Power Point Tracking (MPPT) technique to capture the maximum possible power [5]. Typically, the speed of the wind and the intensity of solar radiation are not always constant, as they are influenced by weather conditions. Therefore, due to the inherent variability of solar and wind electricity generation, the use of storage devices is crucial in maintaining stability between the power production and consumption positions, particularly in Stand-alone Systems where there is no grid connection. Batteries serve as storage devices. In certain circumstances, there may be a lack of wind or low wind conditions, rendering wind power ineffective. Similarly, solar power is non-operational during nighttime hours. In this scenario, the battery fulfills the load requirements. Additionally, when there is a high power output from the Wind generator or PV, the battery gets charged while still meeting the load demands.

The primary criteria in stand-alone systems are to meet customer satisfaction by effectively regulating the inverter operation to provide a consistent output of voltage and frequency. Voltage variations at the point of common coupling (PCC) are caused by changes in load. In distribution systems, the loads are typically unbalanced in nature, especially in 3-phase loads. This unbalance in loads leads to an unbalanced voltage at the PCC [4, 5]. Therefore, the issues related to power quality (PQ) can be minimized through effective regulation of the inverter [8-10].

2.0 Description of the System

Several authors have described and studied independent systems in different works. The next section examines the important topics and presents novel systems that address the issues found in current systems. The present part is subdivided into four distinct segments, which are outlined in the subsections that follow:

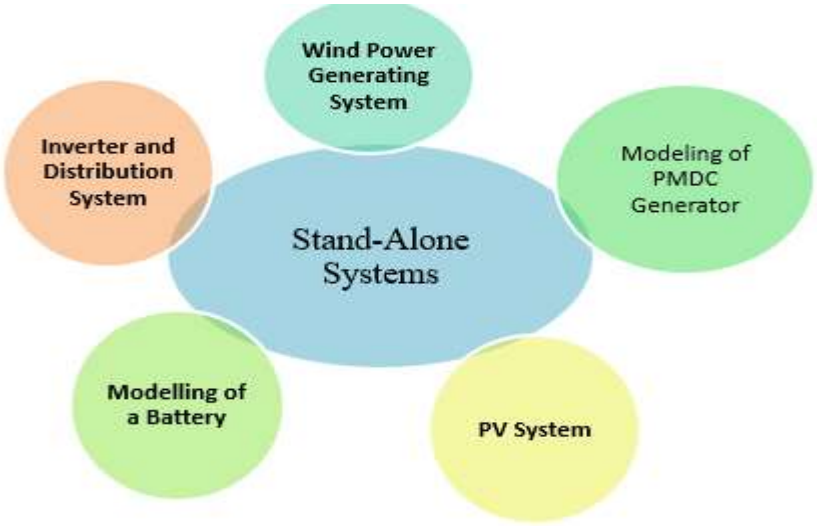

Figure 1.0 Classification of Stand-alone system

2.1 Wind Power Generating System

The equations listed below are used in this framework to simulate a typical windy generator:

$$P_t = 0.5\rho A C_p(\lambda,\beta)v^3 \qquad (1)$$

In the given equation, β represents the density of the air, v represents the speed of the wind, A represents the area swept by the blade, and Cp represents the power coefficient of the turbine rotor.

$$T_m = \frac{P_t}{\omega_t} \text{ And } \lambda = \frac{\omega_t}{v} \qquad (2)$$

In order to achieve optimal power tracking, it is necessary to maintain an equilibrium.

$$\frac{\omega_{t1}}{v_1} = \frac{\omega_{t2}}{v_2} \quad (3)$$

Furthermore, while the wind energy conversion system is operating under maximum power point tracking (MPPT) in a stable condition, the power coefficient (Cp) remains constant at 1 per unit (1p.u.), while the values of voltage (U) and current (A) remain constant.

$$\therefore T_m \alpha = \frac{v^3}{\omega_t} \text{ Therefore, finally, } \frac{T_{m1}}{T_{m2}} = \frac{v_1^2}{v_2^2}$$

In order to create electrical power, it is necessary for the wind turbine to connect the generator. Typically, DFIG or PMSG are the most commonly used in wind generating systems. In references 1 and 2, the authors examined a system based on Doubly Fed Induction Generator (DFIG). In references [4-5], the authors examined the advantages of PMSG and explored the potential of using a PMSG-based electrical power production system. Nevertheless, the aforementioned systems [1-5] are designed for high power applications and require additional converters to establish a connection between the systems and the inverter. In references [4-5], the authors employed a rectifier to convert alternating current (AC) electricity into direct current (DC). By utilising a diode rectifier, the harmonics are introduced into the system. However, the planned filters may not function well due to the fluctuating wind speed, which leads to fluctuations in the voltage and current of the rectifier's output. These kind of systems will raise the expenses of small-scale independent hybrid systems designed for domestic applications. Therefore, this research considers the use of a DC generator to provide electrical power when coupled with a wind turbine. Furthermore, in order to minimise losses and increase power production, this research considers the use of a permanent magnet DC (PMDC) generator for modelling purposes. In order to include a Maximum Power Point Tracking (MPPT) system for a wind turbine, a DC to DC converter is installed with a suitable controller. This converter is connected between the Permanent Magnet DC (PMDC) generator and the DC-link of the inverter. This connection is made since the shaft of the wind turbine and the shaft of the PMDC generator are directly linked. Connecting the wind turbine to MPPT will result in more cost-effectiveness.

2.2 Modeling of PMDC Generator

The Persistent Magnet DC Generators (PMDCG) may be viewed as an independently initiated DC brushing motor that maintains a consistent magnetic flux. Most PMDC brushed-motor machines can function as PMDC generators, although they are not specifically designed for this purpose. But they are not ideal for wind turbine generators because the rotating field acts as a brake, causing the rotor to slow down. The DC machinery in question are equipped with a stator that contains rare earth-based magnetic elements, such as Neodymium or Samarium Cobalt. These magnets provide a powerful stator field flux, replacing the need for wrapped coils. Additionally, the machines have a commutator that is coupled to a wound armature via brushes, similar to previous designs [6].

When PMDC motors are utilised as permanent magnet DC generators, they often need to be operated at speeds significantly higher than their rated motor speed in order to generate a voltage close to their rated motor voltage. Therefore, DC machines with low rpm and high voltage are more suitable for functioning as DC generators [6]. An inherent benefit of the permanent magnet DC generator, compared to other types of DC generators, is its rapid response to variations in wind speed. This is due to the presence of a strong and constant stator field [6].

The permanent magnet DC generator is an optimal selection for small-scale businesses wind turbine installations due to its reliability, ability to function at low speeds of rotation, and high effectiveness, particularly in low wind situations, as it has a relatively low cut-in point [6].

Fig. 1 depicts the power generating system being evaluated, with the wind turbine serving as the main driving force. The mathematical model for the dynamics of a permanent-magnet DC generator circuit, taking into account a resistive load, may be obtained using the two equations that follow:

$$\frac{di_{ag}}{dt} = -\frac{r_{ag} + R_L}{L_{ag}} i_{ag} + \frac{k_{ag}}{L_{ag}} \omega_{rpm} \quad (4)$$

Industrial Engineering Journal
ISSN: 0970-2555
Volume : 53, Issue 4, No. 4, April : 2024

The torsion physical dynamics of generator-prime movers may be described using the Newton's second equation of movement.

$$T_{epm} - \left(B_{mpm} + B_{mg}\right)\omega_{rpm} - T_{eg} = \left(J_{pm} + J_g\right)\frac{d\omega_{rpm}}{dt} \qquad (5)$$

The generator's armature current is represented by the variable "ag i". The angular speed of the propeller and generating is denoted as "Z rpm". The armament resistance and inductance of the generator rotor winding are represented by "ag r" and "Lag" respectively. RL represents the load obstruction, ag k is the rear electromotive force (torque) consistent of the power source, Bmpm and Bmg are the coefficient of viscosity movement, and Jpm and Jg are the moments of momentum of the prime mover and generator, respectively.

The wind turbine generates electromagnetism torque, represented as Tepm. The load tension for the main engine is determined by the electromagnetic torque of the generating.

$$T_{eg} = k_{ag} i_{ag} \qquad (6)$$

Thus, one obtains

$$\frac{d\omega_{rpm}}{dt} = \frac{k_{apm}}{J_{pm} + J_g} i_{apm} - \frac{B_{mpm} + B_{mg}}{J_{pm} + J_g}\omega_{rpm} - \frac{k_{ag}}{J_{pm} + J_g} i_{ag} \qquad (7)$$

The statistical framework describing the dynamics of the primary motor circuits is

$$\frac{di_{apm}}{dt} = -\frac{r_{apm}}{L_{apm}} i_{apm} - \frac{k_{apm}}{L_{apm}}\omega_{rpm} + \frac{1}{L_{apm}} u_{apm} \qquad (8)$$

$$\text{and}, \quad \frac{di_{ag}}{dt} = -\frac{r_{ag} + R_L}{L_{ag}} i_{ag} + \frac{k_{ag}}{L_{ag}}\omega_{rpm} \qquad (9)$$

The variable "uapm" represents the amount of voltage supplied via the armature winding of the prime mover. "rapm" and "Lapm" refer to the resistance of the arms and capacitance of the primary mover's rotor winding, respectively.

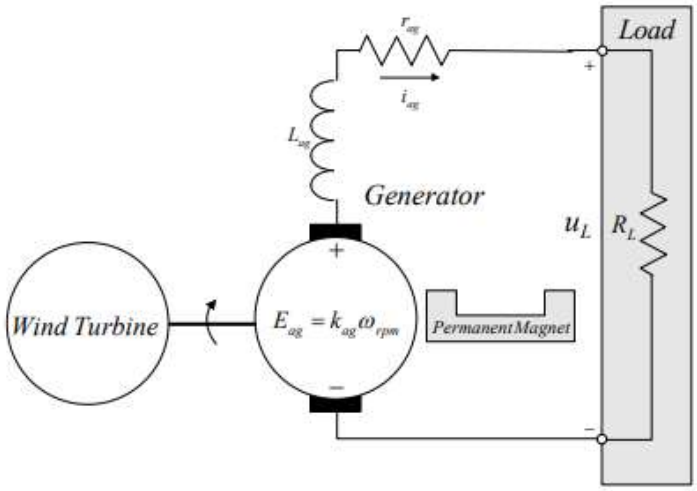

Figure 1.2 shows a schematic layout of a PMDC generating with a wind turbine primary movers.

2.3 PV Circuit

The schematic representation of a photovoltaic (PV) cell is seen in Figure 1.3 A photovoltaic is defined by its current-voltage characteristics functions.

$$I_{PV} = n_p I_{ph} - I_{rs}\left[\exp\left(\frac{q(V_{PV} + I_{PV}R_s)}{AKTn_s}\right) - 1\right] - \frac{V_{PV} + I_{PV}R_s}{R_{sh}} \qquad (10)$$

Let ns represent the total number of cells associated in series, as well as np represent the plenty of cells linked in parallel. The value of q is 1.602•10-19 C, which represents the charge of an electron.

Similarly, K is the Boltzmann constant with a value of 1.3806•10-23 J/K. A is the romantic factor of the p-n junction, which is equal to 2. T represents the temperature of the cell in Kelvin. Iph is the photocurrent of the cell, which depends on the solar irradiation and temperature. Irs represents the reverse saturation current of the cell. G represents the solar irradiance, and VPV represents the voltage of the cell.

Based on the P-V characteristics of a PV system, the PV system may produce the most amount of power at a specific voltage known as the voltage at maximum power point (Vmpp). Figure 3 displays the P-V characteristics for various levels of irradiance, taking into account uniform irradiance. Among the several methods suggested in the literature, the P&O algorithm stands out as the most widely used methodology for Maximum Power Point Tracking (MPPT) [5]. This may be accomplished by the use of power electronics devices, which are employed in power systems [13-25].

The P&O algorithm has the benefit of straightforward implementation in both software and hardware. In this method, the reference voltage (Vmpp) is disturbed in an erratic direction and the electrical power levels of two successive samples are compared. The direction for future perturbation is determined based on the sign of the power change. The feedback loop of control guarantees that the output value closely follows its reference. The subsequent equation is utilised to determine the voltage at which the maximum power point (MPP) is achieved.

$$V_{mpp}(k) = V_{mpp}(k-1) + \Delta V \times \text{sign}\left(\frac{dP_{PV}}{dV_{PV}}\right) \qquad (5)$$

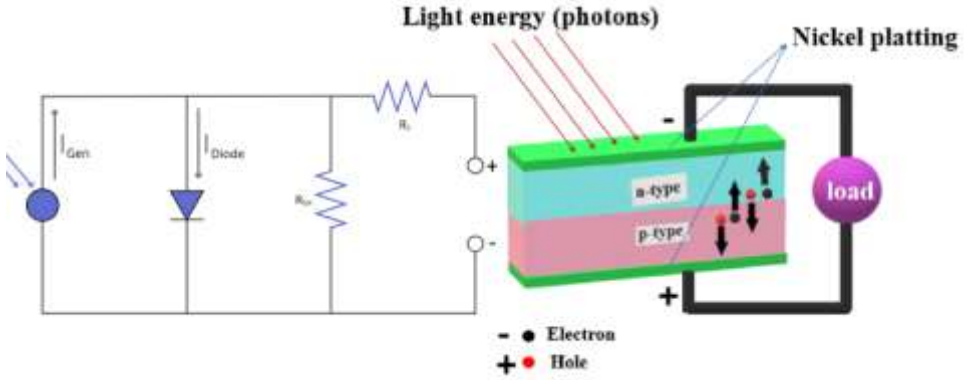

Figure. 1.3: Schematic Diagram of PV Cell.

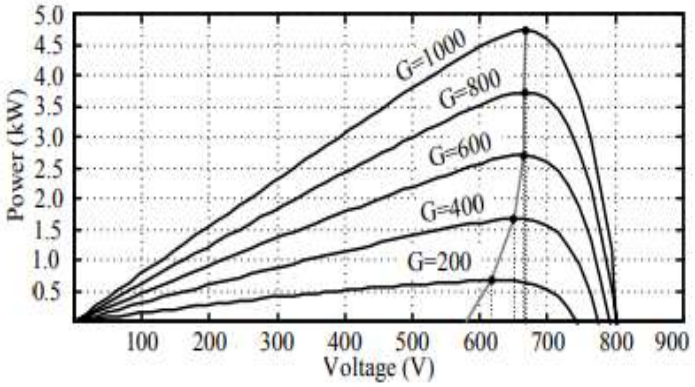

Figure.1.4: P-V properties of a solar energy systems at different irradiances.

2.3 Modelling of a Battery

Portable electronics frequently rely on batteries in order to function. The amount of energy stored in these batteries is restricted. As a result, it is critical to use this energy as effectively as possible in order to maximise battery life. In this study, we define lifespan as the amount of time a battery may be used before becoming empty. It should be noted that with rechargeable batteries, this does not correspond to the amount of time the battery may be used before it stops operating effectively. Of course, the

battery lifespan is mostly determined by the device's energy consumption rate. However, decreasing average usage is not the only technique to extend battery life. The lifespan of a battery is also affected by its usage pattern due to nonlinear physical influences. During periods of heavy energy usage, the effective battery capacity declines, shortening the lifetime. However, during periods of low energy usage, the battery can regain part of its lost capacity, extending its lifespan.

The energy consumption of wireless devices has been investigated using effectiveness models. The models that follow represent the many states that a device can be in, as well as their energy consumption rates. However, these models often just consider energy consumption and do not account for the implications of usage patterns on battery life. To do this, we need to expand the model by integrating it with a battery model. The literature has several battery models. Various methodologies have been used to simulate battery attributes, ranging from very precise electrochemical models to high-level stochastic models. This study provides an overview of the various battery types. These models are assessed for their applicability when combined with a performance model.

The Kinetic Battery Model is one of the versions that has shown to be suitable for this purpose. However, certain changes must be made to adapt the model to the types of batteries utilised in wireless gadgets.

The current investigation implements a general battery model that is provided in references [4-5, 18-19]. In order to enhance accuracy, the temperature variable is also taken into account during the battery modelling process. The model utilises just the state of the battery of charge (SOC) as the state parameter to circumvent the issue of algebraic loops. It can effectively depict four distinct battery chemicals, comprising lead acid batteries.

The modelling is performed by utilising a basic controlled voltage supply with a consistent resistance, as seen in Figure 4. The controlled voltage source is specified by the equations provided underneath.

$$E_m = E_{m0} - K_E(273+\theta)(1-SOC) \quad (11)$$

$$Q_e(t) = Q_{e\_init} + \int_0^t -I_m(\tau)d\tau \quad (12)$$

$$I_p = V_{PN}G_{P0}\exp\left(\frac{V_{PN}}{V_{P0}(\tau_P s+1)} + A_P\left(1-\frac{\theta}{\theta_f}\right)\right) \quad (13)$$

$$C(I,\theta) = \frac{K_c C_{0*} K_t}{1+(K_c-1)\left(I/I^*\right)^\delta},\ K_t = LUT(\theta) \quad (14)$$

$$\text{Where, } SOC = 1-\frac{Q_e}{C(0,\theta)},\quad DOC = 1-\frac{Q_e}{C(I_{avg},\theta)}$$

$$\theta(t) = \theta_{init} + \int_0^t \frac{\left(Ps - \frac{(\theta-\theta_a)}{R_\theta}\right)}{C_\theta}d\tau$$

Where in the world? Em represents the voltage when a circuit has an open state (measured in volts), Em0 represents the open circuit voltage when the battery is fully charged (measured in volts), and θ represents the temperature of the electrolytes (measured in degrees Celsius). Qe represents the charge that has been extracted, measured in ampere-seconds (A S). Qe_init refers to the initial extracted charge, also measured in ampere-seconds (A S). The main branch current is represented by the symbol "Im" (A). The integration time variable is denoted by "τ".

The current loss in the parasitic branch is referred to as "IP", while the voltage at the parasitic branch is represented by "VPN". The parasitic branch time constant is denoted by "τP". The sodium chloride freezing point is represented by the symbol "θf" (0 C).

The empty capacity utilisation at 00 C is denoted by "C0*". The temperature dependent look-up table is referred to as "Kt". The variable "I" represents the nominal battery current, "DOC" represents the depth of charge, "C" represents the battery performance in amperes (A), and "KE," "GP0," and "δ" are standards.

2.4 Inverter and Distribution System

Typically, a 3 phase network is more dependable and consistent for an electricity distribution network. In order to mitigate the reduction in voltage for loads located at a significant distance from the inverter,

this study recommends the use of a three-phase system. The majority of the loads linked to the 3-phase inverter are imbalanced as a result of the single-phase loads in residential homes [15, 18-20, 23-25]. In this scenario, there is an imbalance in the voltage drop across the filter, resulting in imbalanced voltage at the common connection position (PCC) or load bus. The voltage imbalance adversely affects the power quality at the load. To mitigate this impact, a phase voltage controller is integrated into the system to adjust the separate root mean square (RMS) voltages at the point of common coupling (PCC). Figure 5 displays the whole planned architecture.

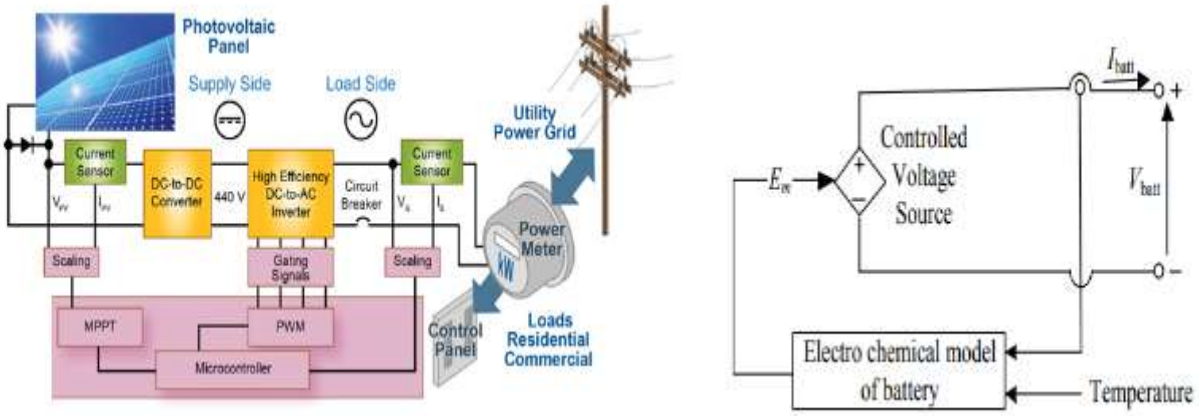

Figure 1.5: General Battery Architecture.

3.0 Controlling of DC Connection Voltages

In order to optimise the power output of a wind electricity source, a direct current (DC) to direct current (DC) converter is installed between the wind generator and the DC link voltage. The power output of the wind generator will change in accordance with the wind speed. Therefore, the output voltage of the PMDC generator will similarly fluctuate. A boost converter is necessary to transmit power from a PMDC generator to the dc link voltage.

The controller will regulate the current of the boost converter in order to run the system at the MPPT point. This may be accomplished by modifying the duty cycle of the boost converter. Furthermore, the direct current (dc) connection voltage is regulated by a dc to dc converter that is connected to the battery. Therefore, the boost converter of the PMDC generator will alone manage the current. Figure 1.7 displays the proposed controller for the PMDC generator's DC to DC converter. The implementation of the perturbed and observe (P&O) algorithm for the maximum power point tracking (MPPT) controller of a photovoltaic (PV) system is depicted in Figure 1.8.

Unbalanced currents in the load cause the superimposition of second order harmonics. The harmonics will induce vibration on the shaft of the wind turbine. In order to mitigate this issue, a novel controller has been introduced for the battery's dc to dc converter, which is a bidirectional converter. This controller has been developed with the assistance of references [4-5] and is depicted in Figure 8(a). The dc-link voltage (Vdc) is passed through a low pass filter to extract the dc component (Vdcc). By subtraction Vdcc from Vdc, the oscillation element (Vdco) may be approximated. The control scheme is now responsible for generating a reference current that must be tracked by the battery current. Two control loops, utilising PI controllers that include are constructed to fulfil two functions: maintaining the dc bus voltage and reducing the second harmonic component of the battery current. This is illustrated in Figure 8(a). The first PI controller takes the error between the desired and actual DC bus voltage, multiplied by a constant, as input to generate a reference current.

The second PI controller utilises the error between the desired and actual DC bus voltage divided by a constant as its input. The reference for the second one is set to '0' in order for the controller to eliminate the oscillating component in the DC voltage. The outputs of both PI controllers are combined to provide the ultimate reference battery current, denoted as *bat I. The acquired reference battery current is compared with the actual battery current (bat I) and the resulting error is analysed using a hysteresis band. This analysis then generates control signals (gating pulses) for the IGBT devices (Q1

Industrial Engineering Journal
ISSN: 0970-2555
Volume : 53, Issue 4, No. 4, April : 2024

& Q2) of the dc to dc conversion.

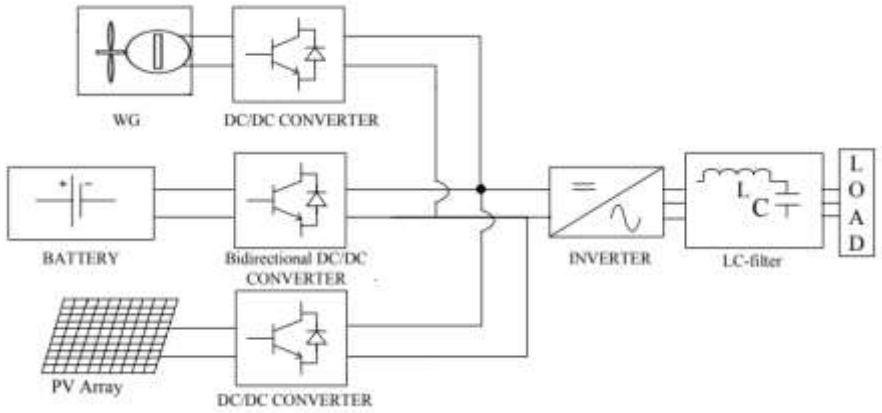

Fig. 1.6: hybrid Stand-Alone Power Production System Using Photovoltaic Wind Energies

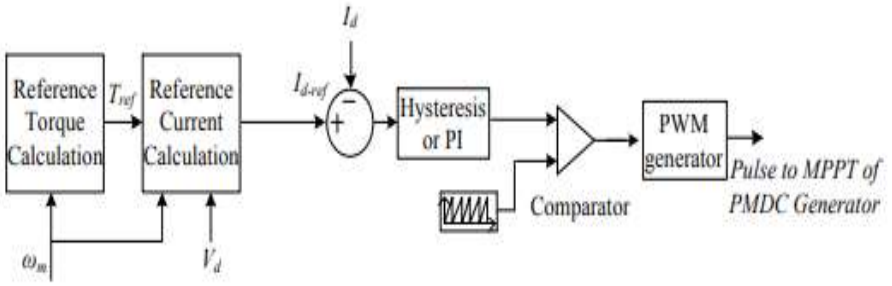

Figure 1.7: the MPPT controller for PMDC generator's DC to DC conversion.

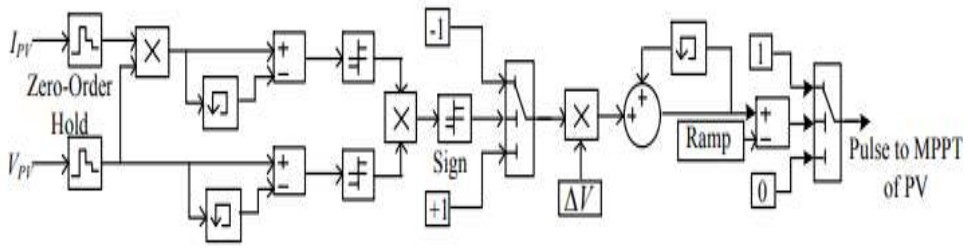

Figure 1.8: MPPT controller for PV system based on P&O

4.0 Transmission Of The Inverter

The inverting regulator is derived from the [4-5]. As previously stated, the majority of the loads linked to a three-phase inverter exhibit an imbalance. As a result of connecting an imbalanced load to the inverter, which the current flowing in every phase will vary, causing an uneven voltage drop between the LC filter utilised in each of the phases. The presence of a voltage imbalance drop will result in the line voltages at the point of common coupling (PCC) being unbalanced. Therefore, it is imperative to rectify the voltage imbalance at the point of common coupling (PCC). In order to accomplish this objective, the discrepancy between the root mean square (RMS) or peak value of the phase voltages at the point of common coupling (PCC) and the desired level of phase voltage is sent into a proportional-integral (PI) controller. The PI controller's output is multiplied by a unit sine wave generator to provide the reference phase voltages (va_ref, vb_ref, vc_ref). PWM impulses are created using va_ref, vb_ref, and vc_ref to control the switching of the load side inverter. The illustration illustrating the control system

5.0 Results

A. The alterations in weather conditions

The plan for the system undergoes testing to assess its performance under varying load power, wind speed, sun irradiation, and temperature conditions. The graphs corresponding to the variations stated

above are displayed in Figure 9. Figure 1.11(a) illustrates the response of the dc-link voltage, whereas Figure 1.11 (b) shows the response of the RMS voltages for specific adjustments. Based on the data presented in Figure 10, it can be concluded that the voltage levels on both the AC and DC sides are sufficient. This achievement can be attributed only to the implementation of the proposed controllers. The current as well as the voltage at the point of common coupling (PCC) are shown in Figure 1.12 (a) and (b) respectively.

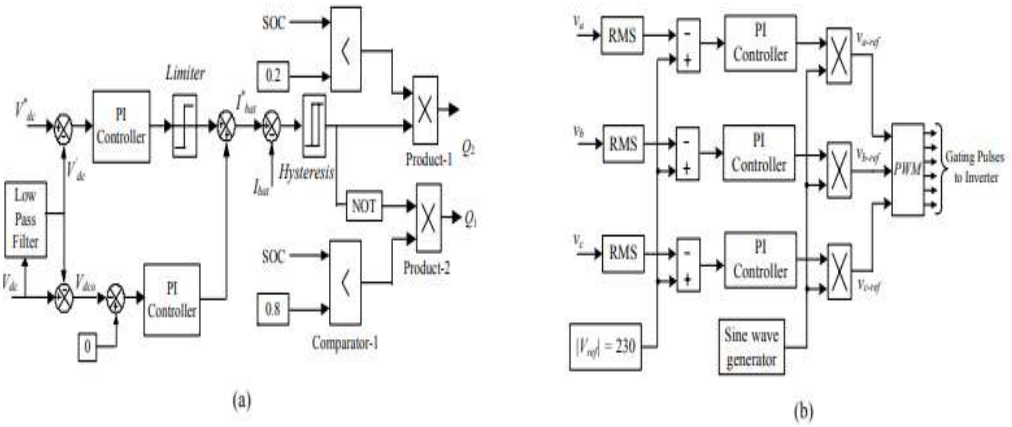

Figure.1.9: (a): Bidirectional converter controller, (b): Inverter Control

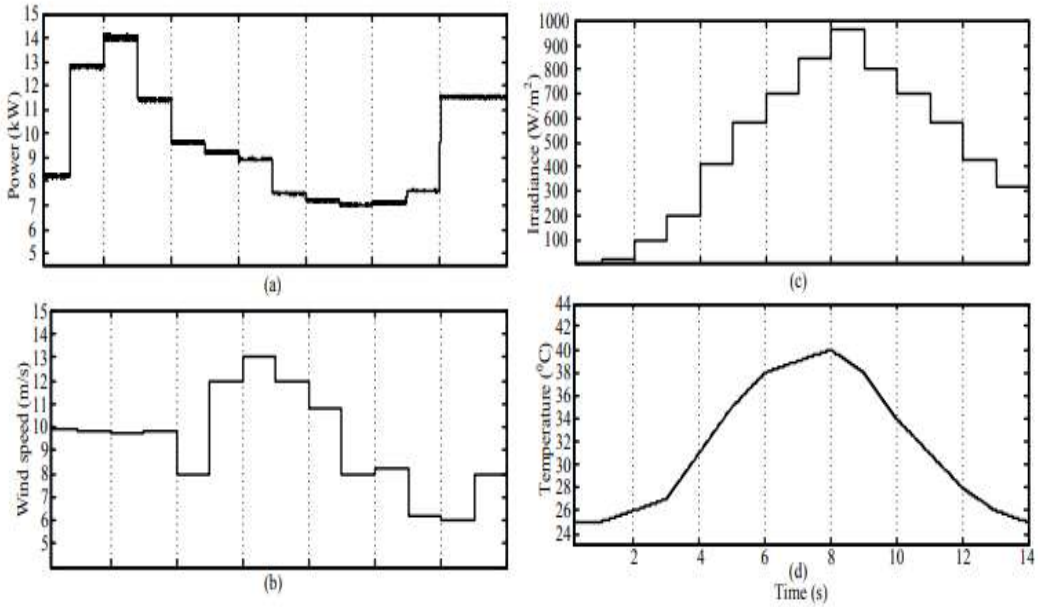

Figure. 1.10: Intermittent changes in load, wind speed, Irradiance and temperature

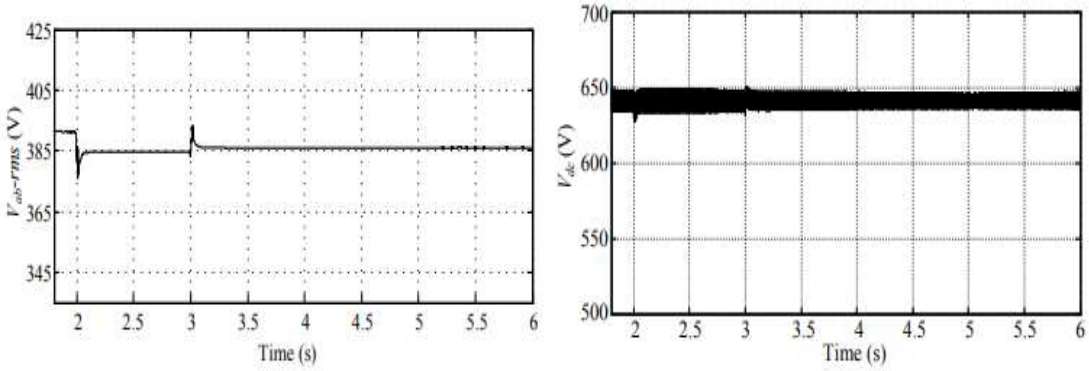

Figure. 1.11: a) RMS output voltage (PCC voltage), b): DC link voltage

Industrial Engineering Journal
ISSN: 0970-2555
Volume : 53, Issue 4, No. 4, April : 2024

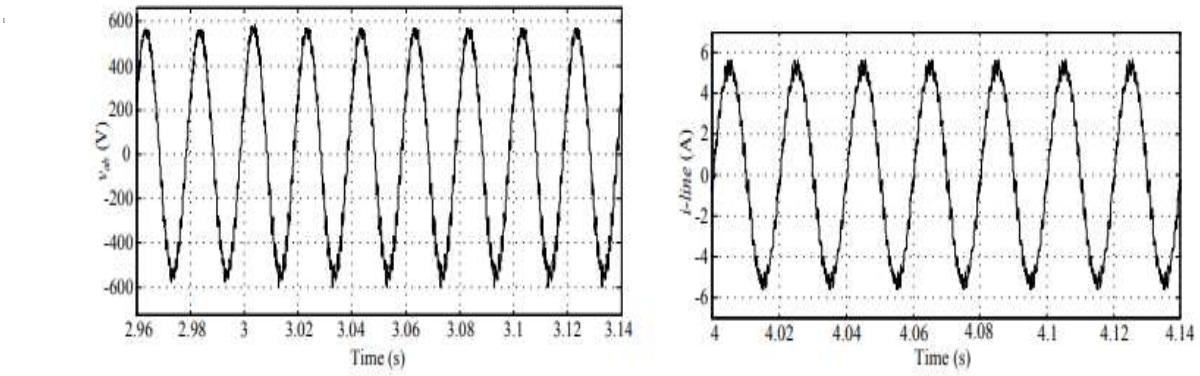

Figure. 1.12: a) Instantaneous output line voltage, b) Instantaneous output line current

B. Consider imbalanced load.

In this scenario, a load that is unbalanced connects at the Points of Common Coupling (PCC). The imbalanced currents of the load in the three different phases (as shown in Figure 12 (a)) are as follows: ila = 3.53 A; ilb = 9.55 A; ilc = 8.45 A. As a result of the uneven flow of electrical currents, there is a decrease in voltage at the L-C filter, causing an imbalance. This imbalance leads to the generation of uneven voltage at the point of common coupling (PCC). The inverter controller ensures that the voltage at the point of common coupling (PCC) is regulated.

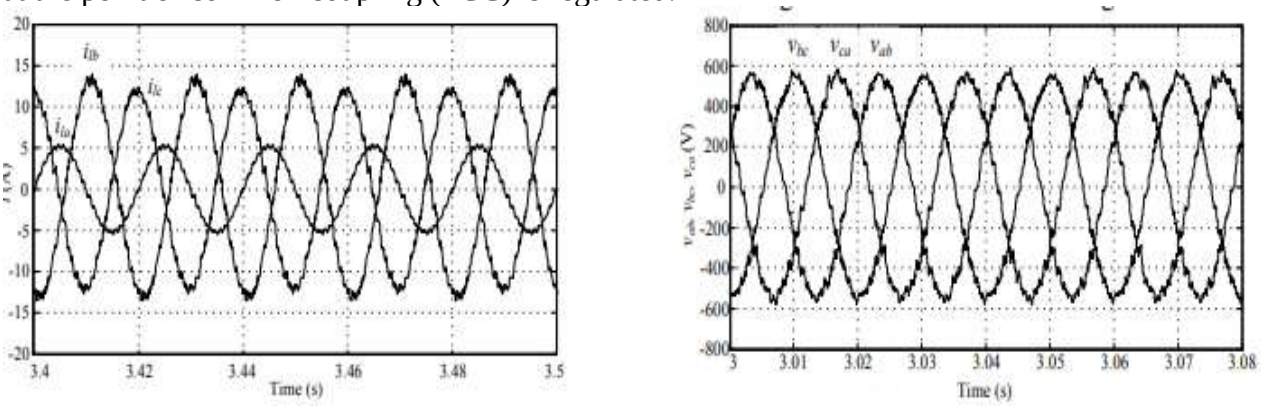

Figure 1.13 a) Displays the three phase currents for an imbalanced load. b) Shows the compensated line voltages at the point of common coupling (PCC).

Although a light load is considered an imbalanced load. The corrected power line voltages for the specified load imbalance situations are displayed in Figure 12 (b). This can be accomplished via the inverter controller that was previously discussed in the preceding section. The inverter controller has the capability to generate varied modulation indexes and voltages in order to maintain balanced voltage at the point of common coupling (PCC).

6.0 Conclusion

This conclusion are presents a hybrid electrical power system for homes that utilises solar and wind energy. The PMDC generator is chosen for windmill generation due to its benefits and advantages. The optimal use of wind and PV systems can be achieved through the effective control of DC to DC converters that are connected to these systems figure 1.8. A bidirectional DC to DC converter is integrated into the system to enhance reliability. The inverter microcontroller is designed to generate balanced energies at the point of common coupling (PCC) even when there is an unbalanced load. This is achieved by producing various modulation indices. The report effectively presents the modelling of all the components utilised in this system. A comprehensive analysis of MATLAB findings is shown as well as addressed under different settings.

References

1.Müller S., Deicke M., and De Doncker Rik W. "Doubly fed induction generator system for wind turbines", IEEE Industry Applications Magazine, May/June, 2002, pp. 26-33.
2.H. Polinder, F. F. A. van der Pijl, G. J. de Vilder, P. J. Tavner, "Comparison of direct-drive and geared generator concepts for wind turbines", IEEE Transactions on Energy Conversion, vol., 21, no. 3, pp. 725-733, Sept. 2006.
3.T. F. Chan, L. L. Lai, "Permanent-magnet machines for distributed generation: a review", Proc. 2007 IEEE power engineering annual meeting, pp. 1-6.
4.C N Bhende, S Mishra, SG Malla, "Permanent magnet synchronous generator-based standalone wind energy supply system", IEEE Transactions on Sustainable Energy, vol. 2, no. 4, pp. 361-373, 2011.
5.S G Malla, C N Bhende, "Voltage control of stand-alone wind and solar energy system", Elsevier, International Journal of Electrical Power & Energy Systems, vol. 56, pp. 361-373, 2014.
6.http://www.alternative-energy-tutorials.com/windenergy/pmdc-generator.ht
7.I.P. Kopylov, Mathematical Models of Electric Machines, Translated from the Russian by P.S. Ivanov, Revised from the Russian edition, 1980. I.P. Kopylov, Mathematical Models of Electric Machines, Translated from the Russian by P.S. Ivanov, Revised from the Russian edition, 1980.
8.Siva Ganesh Malla, D Jaya Deepu, D Pavan Kumar, Jagan Mohana Rao Malla, "Solar powered mobile phone: An innovative experiment", International Conference on Signal Processing, Communication, Power and Embedded System (SCOPES), pp. 1015-1020, 3rd Oct. 2016, India
9.CN Bhende, A Kalam, SG Malla, "Mitigation of Power Quality Problems in Grid-Interactive Distributed Generation System", International Journal of Emerging Electric Power Systems, Vol. 17 Issue:2, pp. 165-172, 1st April 2016.
10. Siva Ganesh Malla, D Jaya Deepu, D Pavan Kumar, "Design and experimental setup of a backup battery as a source to mobile phone battery", International Conference on Electrical, Electronics, and Optimization Techniques (ICEEOT), pp. 2815-2822, 3rd Mar 2016, India.
11. Bose B.K, Power Electronics and Motor Drives, Academic Press, Imprint of Elsevier, 2006.
12. B.L. Theraja, A.K. Theraja, A Textbook of Electrical Technology, Vol.2.
13. Jagan Mohana Rao Malla and Siva Ganesh Malla, "Three level diode clamped inverter for DTC-SVM of induction motor", Joint International Conference on Power Electronics, Drives and Energy Systems (PEDES) and Power India, pp. 1-6, 20-23 Dec. 2010.
14. B. K. Bose, Expert system, fuzzy logic, and neural network applications in power electronics and motion control, Proc. IEEE, vol. 82, pp. 1303–1323, August 1994.
15. Siva Ganesh Malla, JMR Malla, D Jaya Deepu, D Pavan Kumar, "Performance evaluation of DSTATCOM with 9-level GTO converter", International Conference on Electrical, Electronics, and Optimization Techniques (ICEEOT), pp. 4392-4396, 3rd Mar 2016, India.
16. S G Malla, M.Hema Lata Rao, J. M. R. Malla, R. R. Sabat, J. Dadi and M M Das, "SVM-DTC Permanent magnet synchronous motor driven electric vehicle with bidirectional converter", International Multi-Conference on Automation, Computing, Communication, Control and Compressed Sensing (iMac4s)-2013, pp. 742-747, 22-23 March 2013.